# Chapter 6

# Methods for recreating ILC backgrounds: Method B

Three methods of creating a beam to use in conjunction with the FONT module were developed as described in section 5.1 and table 5.1. In this chapter, Method B is discussed.

## 6.1 Methods for creating spray: B

### 6.1.1 Overview

To create a scenario where backgrounds were created in the presence of the main electron beam, Method B was developed. The BPM's measurement of the main electron beam position could be performed with and without backgrounds and the two measurements compared.

The backgrounds were created using thin foils of aluminium placed in the beamline upstream of the module. With a thin amount of material, the beam is only slightly disrupted and the position of the beam can be measured with the striplines as usual. As the electrons pass through the foils, they are deflected by the electric fields of the nuclei and electrons of the foils. Most particles are deflected at small angles and multiple times. There are also bremsstrahlung photons and electrons and positrons from pair production.

The scattered electrons, bremsstrahlung photons and some small numbers of electron-positron pairs, form a halo of particles around the main beam. Figure 6.1 shows the number density per beam charge of the particles hitting the plane with the z location of the front face of the low-Z mask in a GEANT3 simulation of Method B. In this simulation, a foil was placed 12 m upstream and the beam was 800$\mu$m in $\sigma_x$ and 65$\mu$m in $\sigma_y$ and going straight down the centre of the beampipe (x = 0 cm, y = 0 cm). GEANT uses the Molière Bethe formulation of multiple scattering [101] to calculate the passage of the electrons through the material of the foil. Most of the original beam remains in the centre of the beampipe (brown/red) surrounded by a low density halo (light blue). The inner radius of the low-Z mask is marked as a black circle. Those particles in the halo that hit the low-Z mask will go on to cause showers which can produce backgrounds at the location of the BPM striplines.

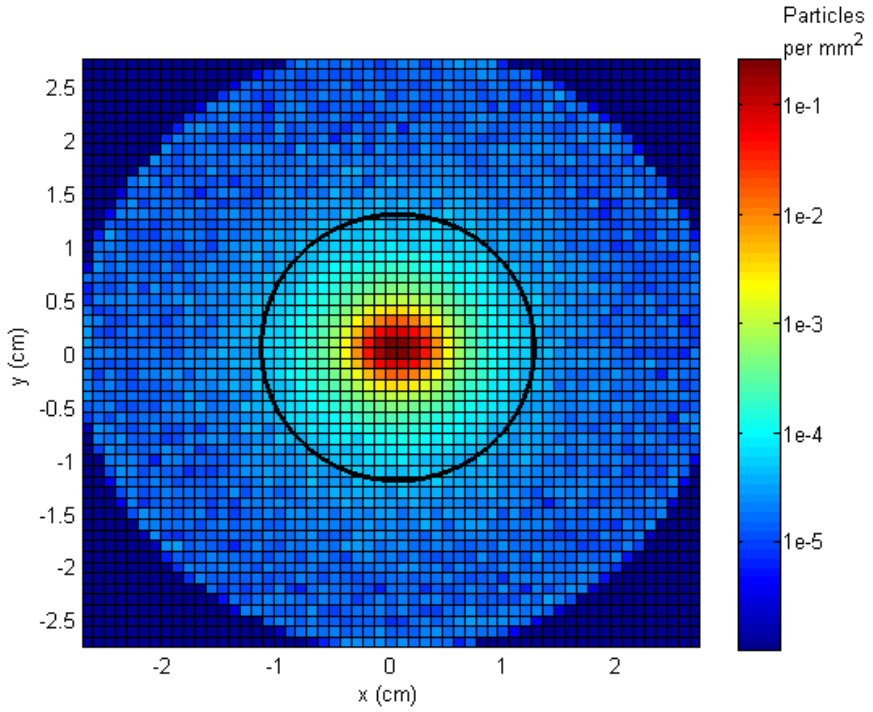



Figure 6.1: The number density of electrons, photons and positrons that hit the front face of the low-Z mask in a simulation of Method B using the 5% foil. The numbers are shown per input electron to the simulation.

### 6.1.2 Designing the experiment

It was important to design the Method B experiment such that enough flux was in the halo of background particles to cause secondary backgrounds at a level similar to those in Method A and those that are expected at the ILC.

To get an indication of the flux that could be expected, a beam of $1 \times 10^6$ 28.5 GeV electrons hitting a thin aluminium foil was simulated in GEANT3. This investigation considered three upstream locations where a foil could be inserted into the beam: 3PR2 and 3PR3 which are profile screens and also the E158 Möller polarimeter[1] (see table 6.1). The flux was estimated between the angles subtended by the front low-Z face of the module (figure 6.2). The further upstream the foil, the higher the flux as most electrons are only scattered through small angles.

The amount of halo that hits the low-Z mask needed to be maximised to increase the secondary backgrounds. The foils were inserted in one of the more upstream positions (using the apparatus formerly used in the E158 Möller experiment) to take advantage of the greater flux of particles at the lower angles. The foil thickness was limited by radiation safety at SLAC to 5% of a radiation length. As the Möller polarimeter apparatus offered the option to use three foils, 3% and 1% radiation length foils were placed in the extra slots in case the backgrounds caused a detectable effect with the 5% foils. The main concern was to bring

[1]The E158 experiment used this device to insert foils into the beamline remotely to measure beam polarisation [102].

| Source | Angle $\theta_2 - \theta_1$ (mrad) | 1% Radiator flux | 3% Radiator flux | 5% Radiator flux |
|---|---|---|---|---|
| 3PR2 | 1.74-0.76 | $0.23 \times 10^{-1}$ | $2.32 \times 10^{-1}$ | $7.68 \times 10^{-1}$ |
| Möller | 2.3-1.0 | $0.18 \times 10^{-1}$ | $1.85 \times 10^{-1}$ | $6.20 \times 10^{-1}$ |
| 3PR3 | 28.9-12.6 | $0.06 \times 10^{-1}$ | $0.76 \times 10^{-1}$ | $2.83 \times 10^{-1}$ |

Table 6.1: The number of hits per electron of beam charge on the low-Z mask in GEANT3 simulations. Three foils are shown (5%, 3% and 1%) at the three upstream locations (3PR2, Möller polarimeter and 3PR3) as shown in figure 6.2.

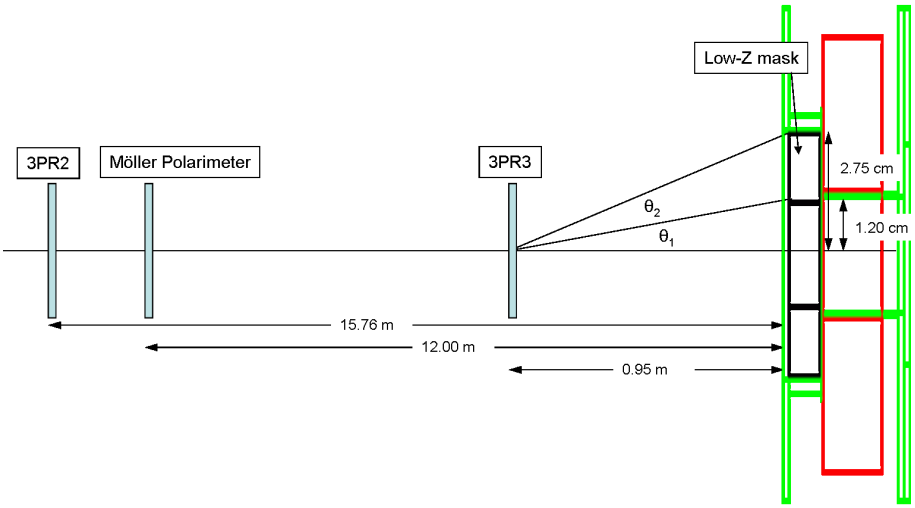



Figure 6.2: The three possible upstream foil positions [103] are shown schematically with the front end of the FONT module. The angles $\theta_1$ and $\theta_2$ as used in table 6.1 are defined and relevant distances given.

| Experiment | Beam Charge (electrons) | Number of BPM stripline hits | Signal height (mV) |
|---|---|---|---|
| Method A (r=1.4cm) | $(9 \pm 1) \times 10^6$ | $(17 \pm 2) \times 10^7$ | 40 |
| 1% Foil | $5 \times 10^9$ | $(2.91 \pm 0.05) \times 10^7$ | $6.8 \pm 0.8$ |
| 3% Foil | $5 \times 10^9$ | $(1.29 \pm 0.01) \times 10^8$ | $30 \pm 3$ |
| 5% Foil | $5 \times 10^9$ | $(2.26 \pm 0.01) \times 10^8$ | $53 \pm 6$ |

Table 6.2: Estimated signal heights based on a comparison of hits of the BPM striplines in GEANT3 simulations and the experimental result of Method A.

the effect of the secondary emission to a level that could be detected in the experiment given the oscilloscope resolution and the inherent jitter of the beam.

To check that this setup was capable of giving a result that could be measured on an oscilloscope with voltage resolution 4 mV, the results of Method A (section 5.3) were used with GEANT3 simulations of Method B. The Method B simulations involved a simulated ESA beam (of 28.5 GeV electrons) as an input to a GEANT3 model of a target made out of aluminium of the appropriate thickness (5%, 3% and 1% $X_0$) followed by 12 m of drift in vacuum and then the GEANT3 FONT module. The numbers of electrons, positrons and photons hitting each stripline in the simulations were evaluated. Comparing the number of simulated particle hits on the stripline in Method A (shown in table 5.3) to the number of simulated particle hits on the stripline in Method B (shown in table 6.2), Method B appears to create a similar level of backgrounds. Using the typical height of signals from Method A (for example, 40 mV as in figure 5.11) and the ratio of simulated particle hits on the stripline in Method A to the simulated particle hits expected on the stripline in Method B, the height of the signal expected for Method B was estimated (table 6.2). The beam charge assumed for Method B was $5 \times 10^9$ electrons because experience with Method A taught that stripline signals from higher beam charges required attenuation before the oscilloscope input.

Based on this estimate for the height of the signal caused by the backgrounds, it would be possible to see the signal due to particles hitting the striplines. However, it was not known how large the beam jitter would be. The position jitter of the beam could obscure such effects and prevent them from being seen despite them being above the resolution of the oscilloscope.

### 6.1.3 Performing the experiment: Method B

This method was used in the March 2007 run at ESA. The 5%, 3% and 1% $X_0$ aluminium foils were placed in the E158 Möller polarimeter, 12 metres upstream of the existing FONT module.

Instrumenting this method only required the standard beam diagnostics available at ESA. The normal beam charge of $1.6 \times 10^{10}$ electrons per bunch was used (with attenuation before the oscilloscope input) and the standard toroid 4140 measured the charge. Special beam

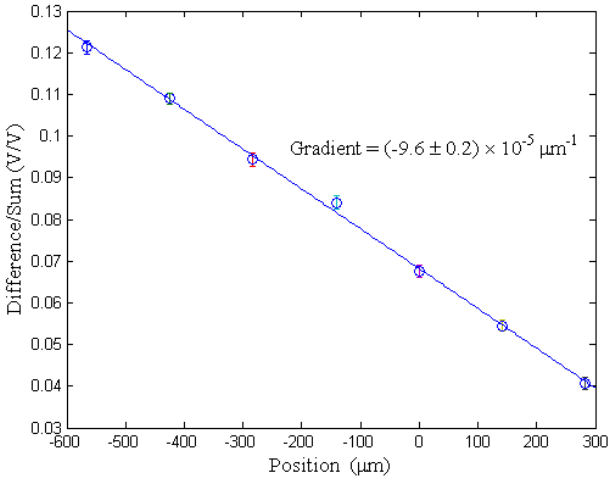



Figure 6.3: The difference between the peak-to-peak voltage of stripline A and the peak-to-peak voltage of stripline C divided by the sum as the beam was moved between the two striplines in 140 $\mu$m steps.

optics were not a concern as a diffuse beam was not required, so existing optics were used that led to a beam at the Möller location of 800$\mu$m in $\sigma_x$ and 65$\mu$m in $\sigma_y$ [97].

The stripline signal heights were calibrated with position[2]. The calibration was achieved by using correctors to translate the entire beam (downstream of the correctors used) in steps of 100 $\mu$m in both x and y. 100 pulses were taken at each point to reduce the effect of the beam jitter. Fourier interpolation was applied to the data to find the most likely values for the maximum and minimum points of the bipolar stripline signal before calculating the difference between two paired (i.e. opposing) striplines and dividing it by their sum. The calibration curve for striplines normalised by charge is shown in figure 6.3.

The calibration with position was also done for the position signals from the FONT4 analogue processors. The processor calibration also used full beam translation. 18 pulses were taken at each point and each difference and sum signal was integrated under (rather than taking their maxima) to remove the effects of oscilloscope trigger jitter and noise in taking a single data point [49]. The calibration curve for the processors is shown in figure 6.4.

The raw stripline signals were attenuated before the oscilloscope to reduce their voltage such that the large voltage signals from $1.6 \times 10^{10}$ electrons could be seen on the oscilloscope. 1000 pulses of stripline signals were recorded using the FONT DAQ with no foil in the beam. Each foil was placed in the beam in turn and 1000 pulses taken. A final set of 1000 pulses was taken without a foil in the beam as a repeat to check for drift.

Two signals from opposite striplines (A and C) were processed using the FONT4 processors to produce difference and sum signals. 1000 pulses of processed signal were recorded for each case: no foil, 5% $X_0$ foil, 3% $X_0$ foil, 1% $X_0$ foil and a repeat of no foil.

With the beam on axis, the background environment for each of the four striplines in the

[2]Stripline signal heights were used, anticipating the need to relate stripline signal amplitudes to position for the background noise.

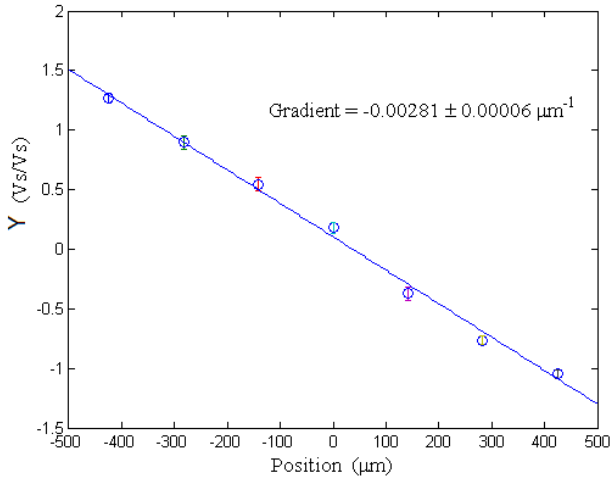



Figure 6.4: The integrated difference divided by sum signal ($Y$, equation 2.2) for the FONT4 analogue processors with inputs from striplines A and C as the beam was moved between the two striplines in 140 $\mu$m steps.

module is identical (by symmetry) and so by taking the difference of the signal from stripline A and stripline C, any effect from the secondary backgrounds is removed. Therefore the difference signal from the processor should be unaffected (with averaging to reduce random fluctuations) unless the subtraction of the signals is done inaccurately. To achieve a difference signal where an effect from secondary backgrounds can be seen, Method B with foils was performed at an offset of 360 $\mu$m as well as with the beam near zero. The offset could not have been too large because it needed to be within the range where the processors produced a linear output for the calibration to hold.

## 6.2 Results: Method B

### 6.2.1 Raw stripline data

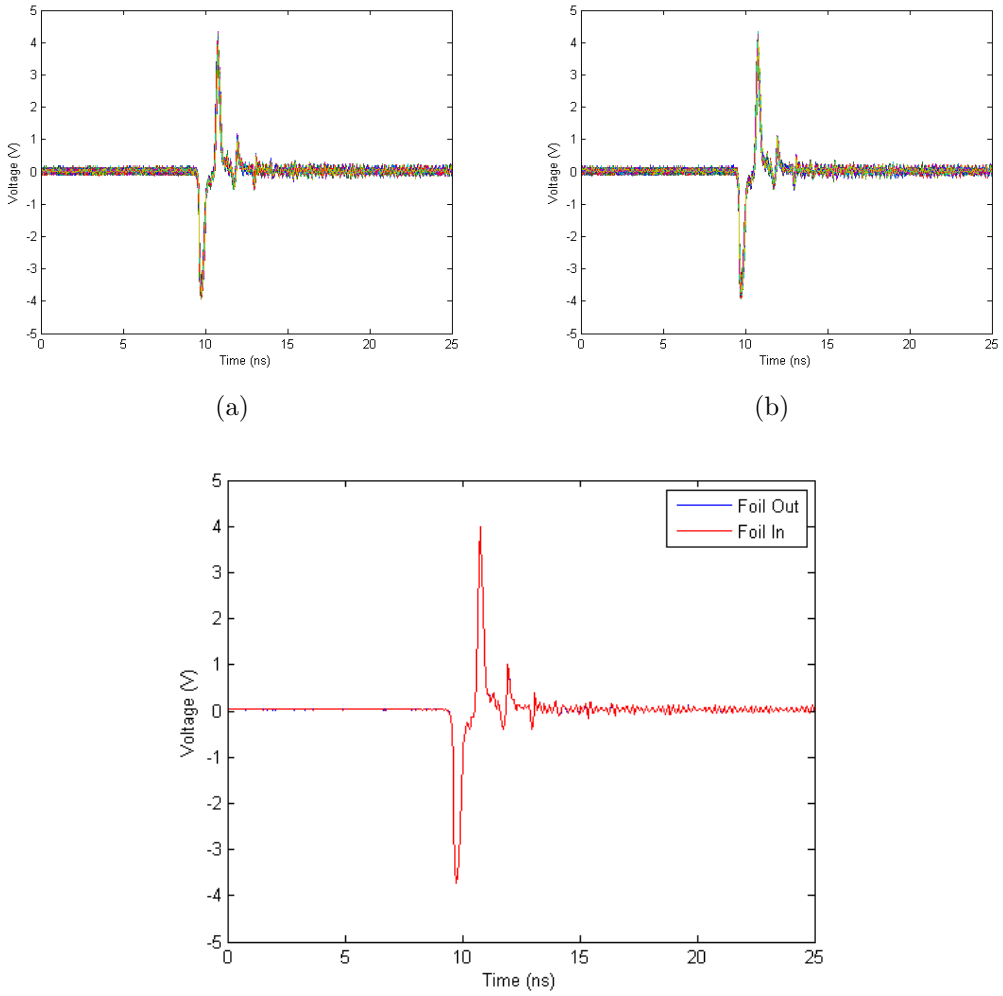
By eye, no change was seen with the foils in the beam and out of the beam (figure 6.5).

The data needed to be analysed, which was done using parameters $m$ and $n$, chosen to be independent of beam charge and position jitter [104]:

$$m = \frac{Q + P}{Q - P} \tag{6.1}$$

$$n = \frac{R}{Q - P} \tag{6.2}$$

Here $Q$ refers to the maximum point of the stripline signal and $P$ refers to the minimum point. $R$ lies half way between the two (if $Q$ occurs at $T_Q$ and $P$ occurs at $T_P$, $R$ occurs at $(T_Q - T_P)/2$). This is shown in figure 6.6.




(a) (b)

(c)

Figure 6.5: The results for 1000 pulses taken with (a) no foil in the beamline and (b) the 5% foil in the beamline. The mean stripline signals are overlaid in (c) where blue is for no foil in the beamline and red is for the 5% foil in the beamline.

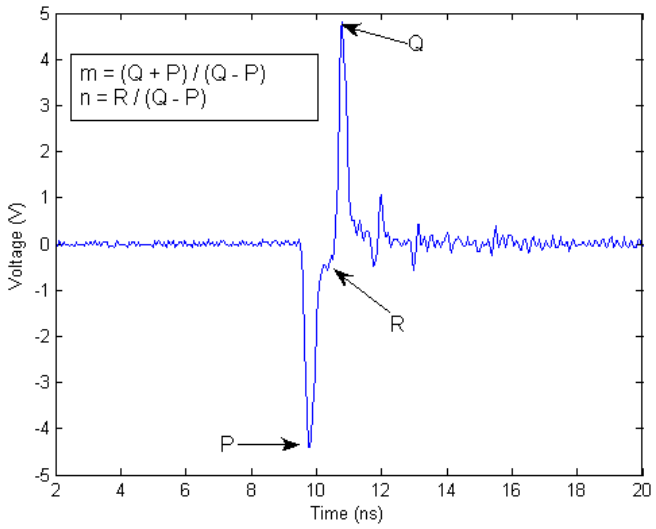



Figure 6.6: The maximum point of the stripline signal ($Q$), the minimum point of the stripline signal ($P$) and the value that occurs at a time exactly half way between those points ($R$).

Both parameter $m$ and parameter $n$ are normalised by the peak to peak height of the bipolar stripline signal ($Q - P$) which is proportional to both charge and position.

The signal from secondary particles, as seen in Method A, involves two negative polarity pulses and a flat part in between (for example figure 5.12). Parameter $n_{\text{in}}$ ($n$ measured with the foil in the beamline) includes the flat contribution to the stripline signal by secondary emission. Parameter $m_{\text{in}}$ ($m$ measured with the foil in the beamline) includes the change in the relative size of the peaks $Q$ and $P$ due to the negative polarity pulses. Parameter $m_{\text{out}}$ ($m$ measured with the foil removed from the beamline) would ideally be equal to zero as $Q$ and $P$ should be equal. However, with real signals this is not often the case due to capacitive and inductive effects.

$m$ is of the most concern to this analysis as a change in stripline signal height would be mistaken as a position offset.

These parameters, $m$ and $n$, were calculated for each stripline signal recorded with the foils inserted into the beamline and each stripline signal recorded with the foils removed. Fourier Interpolation was used to estimate the values that fell between sampling points to minimise the error caused by discrete sampling and the oscilloscope time sampling jitter. The means ($\bar{m}$ and $\bar{n}$) and statistical errors on the means ($s_{\bar{m}}$ and $s_{\bar{n}}$) were calculated. These are shown in table 6.3.

The difference between $\bar{m}_{\text{out}}$ and $\bar{m}_{\text{in}}$ is less than the statistical error on either mean:

$$\Delta\bar{m} = \bar{m}_{\text{out}} - \bar{m}_{\text{in}} < s_{\bar{m}} \tag{6.3}$$

The 5% foil produced the greatest secondary backgrounds but here $\Delta\bar{m} = 0.0001$ with $s_{\bar{m}} = 0.0005 (> \Delta\bar{m})$. Therefore no change in $m$ was observed when the foils were inserted.

| Foil thickness | $\bar{m}$ | $s_{\bar{m}}$ | $\bar{n}$ | $s_{\bar{n}}$ |
|---|---|---|---|---|
| No Foil | 0.0364 | 4.46e-4 | -0.0326 | 1.85e-4 |
| 5% | 0.0363 | 4.79e-4 | -0.0325 | 1.87e-4 |
| 3% | 0.0376 | 4.35e-4 | -0.0324 | 1.87e-4 |
| 1% | 0.0375 | 4.39e-4 | -0.0321 | 1.78e-4 |
| No Foil (repeat) | 0.0378 | 4.55e-4 | -0.0320 | 1.75e-4 |

Table 6.3: The means of the parameters $m$ (equation 6.1) and $n$ (equation 6.2) as calculated for the stripline signals. The statistical errors on the means (given 1000 pulses were taken) were also calculated ($s_{\bar{m}}$ and $s_{\bar{n}}$). A repeat measurement was taken for no foil being inserted in case of drift over time. The data were taken in the order presented in the table.

The same is true for $\bar{n}_{\text{out}}$ and $\bar{n}_{\text{in}}$:

$$\Delta\bar{n} = \bar{z}_{\text{out}} - \bar{n}_{\text{in}} < s_{\bar{n}} \tag{6.4}$$

The 5% foil produced $\Delta\bar{n} = 0.0001$ with $s_{\bar{n}} = 0.0002$. Therefore no change in $n$ was observed when the foils were inserted.

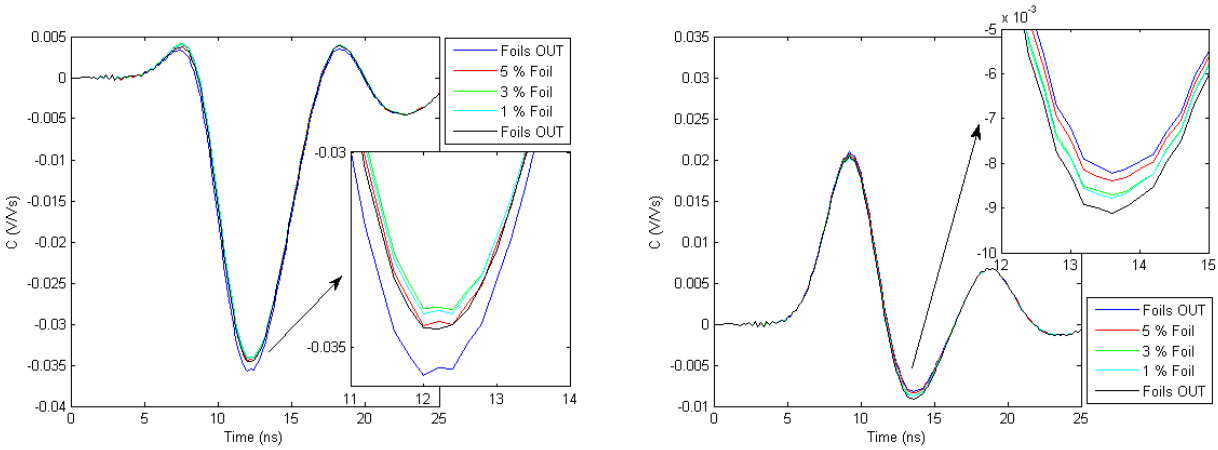
There is some drift observed between the start of this data taking run and the end so the $\bar{m}_{\text{out}}$ and $\bar{n}_{\text{out}}$ are chosen to be from the first "no foil" run, closest in time to 5% foil run.

Although no difference was observed with the foils in and the foils out, the experimental errors offer an upper limit on $\Delta\bar{m}$ and $\Delta\bar{n}$ of 0.0008 and 0.0003 respectively at the 95% confidence level. The limit on $\Delta\bar{m}$ can be used to judge the effect of the secondary backgrounds at the ILC (which is done in section 6.3.1).

### 6.2.2 The processed signals

Signals from the FONT4 analogue processors were examined with foils in and out of the beam. This was done twice for two beam offsets: a small offset (360 $\mu$m) and near zero (70 $\mu$m).

Figure 6.7 shows the processed signal for the initial run without foils (blue) and the runs with the foils in the beamline (red, green and cyan). In both cases, the charge normalised difference signal $C$ (equation 6.5 with the difference signal $V_{\text{Difference}}$ and the sum signal $V_{\text{Sum}}$) is plotted versus time. There appeared to be a change in the processor signals when the foils were inserted. However, there was also a change between the two runs without foils (blue and black) indicating that there was drift during the course of the data. Also, the pattern in processor signals does not agree with the 1% foil causing the lowest backgrounds (and hence causing a signal similar to that of the no foil runs) and the 5% foils causing the highest backgrounds (and hence causing a signal with the greatest difference to that of the no foil runs). This is true for both beam positions: near zero (where the effect from background particles only appears in the sum and so should not cause a noticeable change in processed signal) and at 360 $\mu$m.




(a) Beam offset by 360 $\mu$m

(b) Beam near the beampipe centre

Figure 6.7: $C$ (equation 6.5) versus time, averaged over 1000 pulses. The data are shown for no foils in the beamline (blue and black), the 5% foil in the beamline (red), the 3% foil in the beamline (green) and the 1% foil in the beamline (cyan). The data were taken in the order shown in the legend.

$$C = \frac{V_{\text{Difference}}}{\int V_{\text{Sum}}\, dt} \tag{6.5}$$

The processed signals were expressed as a single dimensionless value $D$:

$$D = \frac{\int V_{Difference}\, dt}{\int V_{Sum}\, dt} \tag{6.6}$$

This is the integrated difference divided by the sum. This removed the effect of charge jitter. It was calculated for each processed signal recorded with the foils in the beamline and for each processed signal recorded with the foils removed from the beamline. The mean ($\bar{D}$) and error on the mean ($s_{\bar{D}}$) was calculated for each foil (or no foil) case. These values are shown in table 6.4 and table 6.5.

The near zero data shown in table 6.4 shows a trend that resembles drift confirming what was seen in figure 6.7(b). Near zero, it was not expected that there would be any effect from the foils unless the stripline signals were processed in an unexpected way through the electronics. The data support that there was no effect from the foils that could be seen due to the drift between the two runs without foils. From these data, $\bar{D}$ changes by 0.035 between the first run without a foil and the final run without a foil.

With the beam at a small offset of 360 $\mu$m, there appeared to be a large difference in $\bar{D}$ of 0.053 between the data run without the foil at the start of the experiment and the data run without the foil at the end of the experiment (table 6.5). The difference between the first data run without foils and the 3% data run is largest (0.076) however this is unlikely to be due to secondary backgrounds: the pattern does not match the expected order of the 5% foil giving the largest difference followed by 3% and then 1%.

| Foil thickness | $\bar{D}$ | $s_{\bar{D}}$ |
|---|---|---|
| No Foil | 0.317 | 0.002 |
| 5% | 0.307 | 0.002 |
| 3% | 0.294 | 0.002 |
| 1% | 0.290 | 0.002 |
| No Foil (repeat) | 0.281 | 0.003 |

Table 6.4: The parameter $\bar{D}$ (equation 6.6) for the processed position signals when the beam was nearly centred in the BPM. The statistical error on the mean (given 1000 pulses were taken) was also calculated. A repeat measurement was taken for no foil being inserted in case of drift over time. The data were taken in the order presented in the table.

| Foil thickness | $\bar{D}$ | $s_{\bar{D}}$ |
|---|---|---|
| No Foil | -0.942 | 0.001 |
| 5% | -0.873 | 0.002 |
| 3% | -0.866 | 0.001 |
| 1% | -0.869 | 0.001 |
| No Foil (repeat) | -0.889 | 0.001 |

Table 6.5: The parameter $\bar{D}$ (equation 6.6) was calculated for the processed position signals with the beam at a small offset of 360 $\mu$m. The statistical error on the mean (given 1000 pulses were taken) was also calculated. A repeat measurement was taken for no foil being inserted in case of drift over time. The data were taken in the order presented in the table.

No such large drift was seen in the raw stripline data. This could be a change in beam conditions during the data taking with the processors (compared to the stable beam conditions as the raw stripline data was taken) or possibly a drift within the processor, which has never been tested over extended periods of time for stability.

Due to the apparent drift, conclusions cannot be drawn from the data with the processors.

## 6.3 Simulating the experiment: Method B

The GEANT3 description of the module was changed to include an upstream foil to simulate this method. It included a thin foil of aluminium (with thickness that varied between 1% and 5% of a radiation length) followed by 12 m of drift as shown in figure 6.8. A Gaussian beam was generated with energy 28.5 GeV and 0.2% spread, 1000 $\mu$m in $\sigma_x$, 100 $\mu$m in $\sigma_y$ and 500 $\mu$m in $\sigma_z$. $10^6$ particles were used in the simulation and tracking was enabled down to 100 eV using the modified GEANT.

The outgoing beam at ESA was 28.5 GeV, well below the ILC electron energies. This does not affect the stripline signal from the main beam as the electrons are still relativistic [43] so the main stripline signal is identical to an outgoing beam signal at the ILC if beam charge is matched. The energy distribution of the scattered electrons from the foils is also many orders of magnitude low (see figure 6.9) but thanks to matching the materials in the IR,

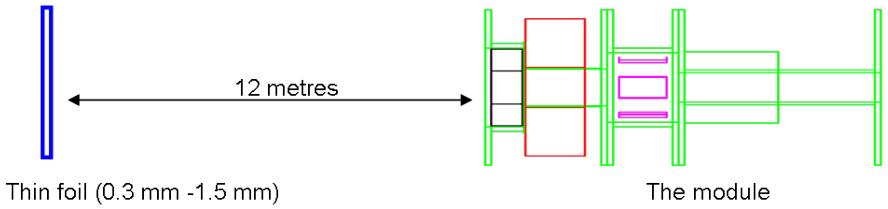



Figure 6.8: The FONT module with a thin target upstream. Green represents iron, black is carbon and red is lead. The BPM striplines are highlighted in purple and modeled to be made from iron. This is not to scale.

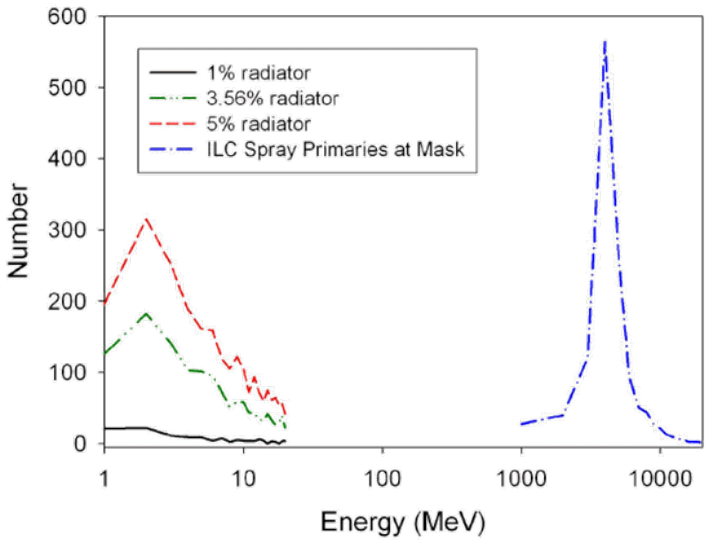



Figure 6.9: The energy spectra of the electrons in the beam halo after being passed through foils (shown in red, green and black) and the energy spectrum of the pairs from the ILC IP that hit the low-Z mask (blue) [105].

what actually hits the BPM striplines has a very similar energy distribution according to GEANT3 simulations shown in figure 6.10. The number of particles hitting the strips shown here is from a simulation with $10^6$ electrons. The beam charge in Method B was $1.6 \times 10^9$, therefore the number of particles in Method B exceeds ILC numbers by approximately three orders of magnitude.

As with Method A, the percentage of hits on the striplines from photons was slightly different for Method B simulations compared with ILC simulations (table 6.6). 91% of the hits on the striplines in Method B were photons compared to ∼80% for the striplines at the ILC.

### 6.3.1 Using GEANT3 Simulations to scale from ESA to ILC

The Method B results put limits on parameters $\Delta\bar{m}$ and $\Delta\bar{D}$. It is necessary to interpret these limits into position errors caused by noise on the striplines from backgrounds at the ILC.

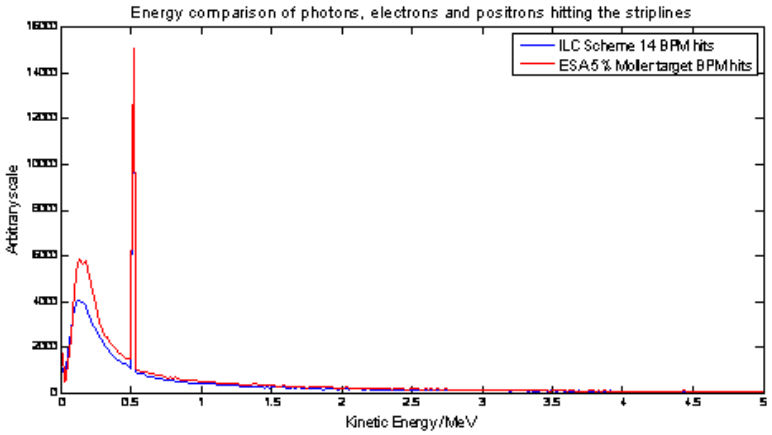



Figure 6.10: The energy distribution of the GEANT3 ILC simulation hits on the striplines (blue) and the energy distribution to the hits on the striplines with the 5% foil at ESA (red). Here electron, positron and photon hits are included, the peak at 0.511 MeV being photons from annihilation (in both curves).

| | ILC % of total hits | | | | Method B % of total hits |
|---|---|---|---|---|---|
| | 1 | 2 | 3 | 4 | A,B,C,D |
| Electrons | 10 | 14 | 10 | 15 | 6 |
| Positrons | 7 | 8 | 6 | 7 | 3 |
| Photons | 83 | 78 | 83 | 78 | 91 |

Table 6.6: The percentage of electron, positron and photon hits on each stripline for Method B compared with the percentages for ILC feedback BPM striplines. Due to the symmetry of Method B, the striplines are identical. The ILC striplines are assigned numbers as shown in figure 3.24(a).

| | 5% foil | 3% foil | 1% foil |
|---|---|---|---|
| Electron hits | $(2.71 \pm 0.02) \times 10^{-3}$ | $(1.39 \pm 0.01) \times 10^{-3}$ | $(3.54 \pm 0.09) \times 10^{-4}$ |
| Positron hits | $(1.51 \pm 0.01) \times 10^{-3}$ | $(7.88 \pm 0.08) \times 10^{-4}$ | $(1.8 \pm 0.1) \times 10^{-4}$ |
| Photon hits | $(4.10 \pm 0.02) \times 10^{-2}$ | $(2.36 \pm 0.01) \times 10^{-2}$ | $(5.3 \pm 0.1) \times 10^{-3}$ |

Table 6.7: The number of particle hits on each stripline for Method B per electron of beam charge. Each stripline is identical due to azimuthal symmetry.

### Scaling the stripline study result $\Delta\bar{m}$

$\Delta\bar{m}$ is a charge normalised parameter of the difference between a stripline with additional noise from secondary backgrounds and the same stripline without additional noise from secondary backgrounds.

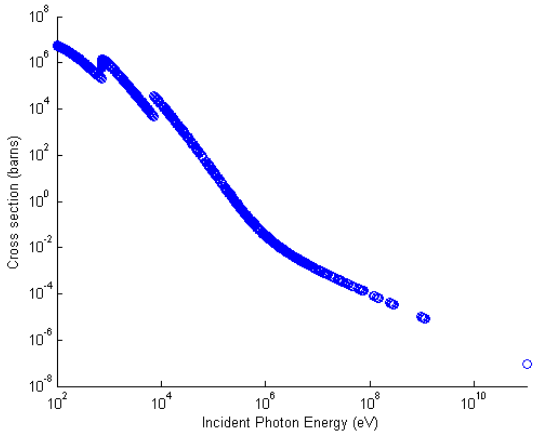
Simulations were used to determine a scaling factor to relate Method B to the ILC. Through GEANT3 simulations of Method B, it is possible to express the secondary backgrounds that cause $\Delta\bar{m}$ as a number, based on the particle hits on the Method B stripline. It is also possible to do the same for the ILC 14 mrad crossing angle simulations (section 3.4.4) and then to scale the Method B results with the ratio of the secondary backgrounds in Method B to the secondary backgrounds expected at the ILC.

To proceed with scaling from ESA Method B to ILC, GEANT3 simulations were repeated with the beam parameters measured during the experiment (as stated in table 5.1). The number and energies of electrons, positrons and photons hitting the striplines were recorded as shown in table 6.7. The number of particles hitting the striplines was used as the measure of how noisy the BPM environment was in both the ESA and ILC case.

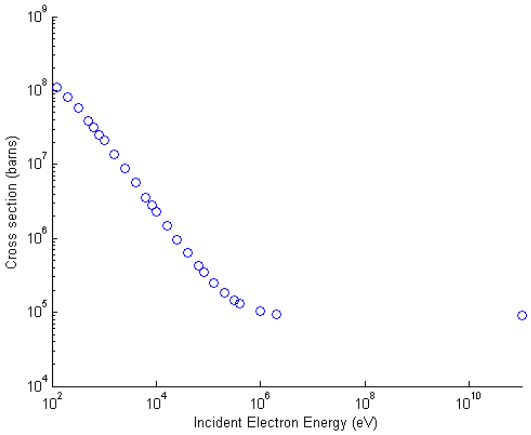
According to the 5% foil simulation, per input electron there were $(2.71 \pm 0.02) \times 10^{-3}$ electrons, $(1.51 \pm 0.01) \times 10^{-3}$ positrons and $(4.10 \pm 0.02) \times 10^{-2}$ photons hitting each stripline.

The total number of hits (electrons, positrons and photons) cannot be reliably used as an indicator for how conditions at ESA compare to ILC because the percentage of hits that are photons at ESA is greater than the percentage of hits that are photons at the ILC (as shown in table 6.6) and charged particles and photons interact with matter in different ways. Cross section data for interactions with electrons and photons were gathered from the Lawrence Livermore Evaluation Electron Data Library [106] and Evaluated Photon Data Library [107] respectively. Each particle that hit the striplines was weighted by the cross section of its interaction with iron (the material of the striplines) given its kinetic energy. The interactions with the greatest cross section at these energies was ionisation through an incident photon or electron with cross sections shown in figure 6.11. Only interactions that resulted in secondary emission and hence a signal on the stripline were considered. Interactions with all atomic sub-shells were considered plus pair production, the cross sections found through log-log interpolation and summed together to give the overall cross section. This gave each particle hit[3] a weighting that could be summed across the types of particles producing one number that could be used to compare the ILC and ESA BPM conditions and scale the results.

[3]Positrons interactions were treated using the electron interaction data.




(a) Cross section for the total photoionisation of Fe with incident photon energy.




(b) Cross section for the ionisation of the Fe 4s subshell with incident electron energy.

Figure 6.11: Cross sections for particle interactions for iron from the Lawrence Livermore Evaluation Electron Data Library [106] and Evaluated Photon Data Library [107].

Using the cross section weighting to particle hits, the 5% foil case is characterised by $2.86 \pm 0.03 \times 10^3$ barns.

In the ILC 14 mrad scheme 14 simulation with anti-DID, there were different numbers of hits on each stripline (see table 3.2). Since the position is calculated using the "Difference/Sum" method, it is the imbalance between a stripline pair that is of interest, specifically the top and bottom striplines since feedback is in y. The ILC simulations indicates that per input electron, there is an imbalance between the top and bottom striplines of $(0.7 \pm 2.2) \times 10^{-7}$ electrons, $(2.2 \pm 1.1) \times 10^{-7}$ positrons and $(1.7 \pm 1.0) \times 10^{-6}$ photons. Using the cross section weighting to particle hits, the ILC case has a top strip characterised by $9 \pm 1$ barns and a bottom strip $7.5 \pm 0.5$ barns giving a maximum imbalance of 3 barns.

The 5% foil case is therefore 990 times worse in terms of particle hits.

The striplines were calibrated using the Difference/Sum method (figure 6.3). At the ILC, 1 micron resolution is required. Therefore, in Method B, since it is 990 times worse, the signal caused by hits on one of the BPM striplines needs to be less than 990 $\mu$m after the calibration is applied for this resolution to be satisfied.

$\Delta\bar{m}$ as defined in equation 6.3 is in units of dimensionless pickup radius (it is a charge normalised difference between two striplines). The measurement of $\Delta\bar{m}$ was limited by experimental errors and is therefore less than $s_{\bar{m}} = 0.0008$. Given the calibration constant in figure 6.3, this upper limit corresponds to a position of 8.5 $\mu$m. This is approximately a factor of 100 below the value that suggests a problem for the ILC stripline BPM. In ILC backgrounds, 990 times smaller than Method B backgrounds, the effect of the pair backgrounds would therefore be to create a signal on the stripline BPM that causes errors below 8.6 nm.

### Scaling the processor study result $\Delta\bar{D}$

The FONT4 analogue processors use the difference between two stripline inputs and so it is not possible to look at the noise on just one stripline in the data as above.

The GEANT3 simulation with the 5% foil in place was repeated for a small beam offset of 360 $\mu$m. For each input electron there was an imbalance of hits between the stripline that was targeted and the opposite stripline. The imbalance came to $(2.0\pm0.8)\times10^2$ hits with the simulation being run four times and the results averaged. With the cross section weightings, one of the two strips used with the processor is characterised by $(2.34\pm0.06)\times10^3$ barns and the other $(2.18\pm0.02)\times10^3$ barns. This gives a maximum imbalance of 80 barns compared to the imbalance of 3 barns for the ILC.

The 5% foil case is therefore producing 28 times the imbalance on the striplines than worst imbalance in the ILC case. Thus if the position resolution of the processor is degraded by 28 $\mu$m, there is a concern for the 1 $\mu$m resolution target at the ILC.

The greatest difference observed in the parameter $\bar{D}$ ($\Delta\bar{D}$) was between the first run without foils and the run with the 3% foil. Here, $\Delta\bar{D} = 0.076$. This is a position measurement of 27 $\mu$m from the integrated difference/sum calibration (figure 6.4) and therefore only just below the 28 $\mu$m level of concern. However, the observed $\Delta\bar{D}$ is unlikely to be due to the presence of backgrounds. This would be a borderline concern if it was due to the backgrounds but the drift between the first run with the foils out and the repeat run indicates that it is not.

## 6.4 Summary to Method B

A method was developed to produce backgrounds at the location of the BPM in the FONT module in the presence of the main beam. This created a situation where the beam position could be measured with and without backgrounds present.

The backgrounds were created by using thin aluminium foils upstream of the module. With a foil 5% $X_0$ placed 12 m upstream of the module, secondary backgrounds on a stripline were $\sim 990$ times worse than the imbalance of secondary backgrounds between the top and bottom striplines at the ILC. The effect of the secondary backgrounds on the stripline was investigated. This study indicated that position resolution errors at the ILC due to the beam-beam pair background was less than 8.6 nm.

The investigation with the FONT4 analogue processors did not lead to any conclusions since large drift was observed in the data masking effects of the backgrounds.

Method B indicates that the backgrounds at ILC in the worst case scenario postulated (accelerator parameters scheme 14 and an untuned anti-DID) do not cause enough noise on the striplines to affect micron-level resolution.